

An Update on the Banana Effect

D. Schulte, CERN, Geneva, Switzerland

Abstract

Wakefield effects in the main linac of a future linear collider can strongly affect the beam-beam interaction at the collision point and potentially lead to a significant luminosity loss. This paper gives an update on the status of the simulations of this effect.

1 INTRODUCTION

Future linear colliders require very small beam sizes at the interaction point (IP) in order to achieve high luminosity. The small size of each beam leads to the creation of very intense electro-magnetic fields which focus the oncoming beam, leading to strong beam-beam interaction. For most simulations so far, the particle distributions of the beams were treated as being completely uncorrelated in the 6-dimensional phase space. However correlations exist, especially between the transverse and longitudinal particle positions—for example introduced into the beams by static imperfections in the main linacs. It was found that taking into account these correlations can strongly modify the beam-beam interaction [1]. In TESLA a very small emittance increase of 1% can lead to a significant loss in luminosity (20%), if the beam-beam collisions are not optimised. This effect is sometimes referred to as the banana-effect due to the visual appearance of the phase space that the bunch occupies. Based on a single case, the reference showed that it may be possible to, at least partly, recover the luminosity by optimising the collision angle and offset. In the framework of the International Linear Collider Technical Review Committee [2] a more quantitative estimate of the effect is necessary, and is given below. Four different machines are considered by the review committee: TESLA, JLC-X, NLC and CLIC. Another design, JLC-C, is partially covered. Since the beam properties of NLC and JLC-X are very similar only TESLA, NLC and CLIC are considered in the following.

Not only static imperfections are of concern, but also dynamic imperfections change the beam offsets, the beam angles and the bunch shapes at the IP; the movement of the tunnel floor is a good example. Because of their dynamic nature only limited time is available to correct these effects. Likely, not the full compensation that can be achieved for static imperfections can also be achieved for dynamic ones. A discussion of some dynamic effects is thus included below.

In the following the need to go to strong beam-beam interaction is motivated, then the impact of the banana effect

on a static machine is discussed. Finally some results for the luminosity in the presence of dynamic imperfections follows.

2 BEAM-BEAM INTERACTION

To achieve the required high luminosity, the beams must be focused to very small transverse sizes at the IP. They therefore produce a very intense electro-magnetic field which focuses the other bunch during the collision. The strength of this effect is conveniently described by the disruption parameters $D_{x,y}$

$$D_{x,y} = \frac{2Nr_e}{\gamma\sigma_{x,y}(\sigma_x + \sigma_y)} \quad (1)$$

Here, r_e is the classical electron radius and γ is the beam energy divided by the electron mass; the meaning of the other parameters is given in table 1. For $D \ll 1$ the beam-beam interaction is weak; the beam acts as a thin focusing

symbol	unit	TESLA	NLC	CLIC
N	[10^9]	20	7.5	4
σ_z	[μm]	300	110	35
σ_x	[nm]	554	243	204
σ_y	[nm]	5.0	3.0	1.2
E	[GeV]	250	250	250
f_r	[Hz]	5	120	200
n_b		2820	195	154
Δt	[ns]	337	1.4	0.67
\mathcal{L}_0	[$10^{34}\text{m}^{-2}\text{s}^{-1}$]	3.4	2.1	2.3
P_{beam}	MW	11.3	7.0	4.9
D_x		0.22	0.16	0.04
D_y		24.8	12.8	6.6

Table 1: Some beam parameters at the interaction point of the different machines. N is the number of particles per bunch, σ_x , σ_y and σ_z are the horizontal, vertical and longitudinal Gaussian RMS bunch lengths and E is the beam energy. In the case of CLIC the vertical spot size is obtained by a fit, since due to synchrotron radiation and dispersive effects in the beam delivery system the beam distribution is not very Gaussian. The bunches are delivered in f_r pulses per second each containing n_b bunches with a spacing in time of Δt . In case of NLC and CLIC the luminosities \mathcal{L}_0 are given before subtracting the allowance of 5% and 10% luminosity loss for the tuning of the beam delivery system. TESLA does not foresee such an allowance. The disruption parameters D_x and D_y are calculated using the nominal emittance at the IP, these are in case that the emittance growth is completely uncorrelated.

lens on the oncoming beam. In the case $D \gg 1$ the beam-beam interaction is strong since the particle trajectories are significantly modified during the crossing. Analytic treatment of the beam-beam interaction in this regime is very difficult, if not impossible. For very high D the collision becomes unstable, the well known two-stream instability. Since all colliders have $D_y \gg 1$ simulation of the collision is necessary.

Since the beam-beam forces are focusing, they increase the luminosity by the pinch enhancement factor H_D which is usually of the order of 1.5 or 2. With higher disruption parameters the luminosity enhancement gradually increases. However, the beam-beam collision becomes unstable. Very small offsets can therefore lead to significant loss in luminosity. For this reason, avoiding large D_y would be advantageous. In order to achieve high luminosity, a high disruption parameter is often required. This can be understood by expressing the luminosity as a function of the vertical disruption. The luminosity can be written as

$$\mathcal{L} = H_D \frac{n_b f_{rep} N^2}{4\pi\sigma_x\sigma_y} = \frac{P_{beam}}{E} \frac{N}{4\pi\sigma_x\sigma_y} \quad (2)$$

Here, P_{beam} is the power of one beam. Using $\sigma_x \gg \sigma_y$ one can calculate $N/(\sigma_x\sigma_y)$ from D_y

$$\mathcal{L} \approx H_D P_{beam} D_y \frac{1}{\sigma_z} \frac{1}{8\pi r_e m c^2}$$

Here, m is the electron mass and c the speed of light. Evaluation of the constants leads to

$$\mathcal{L} \approx H_D \times 1.74 \times 10^{34} \text{ cm}^{-2} \text{ s}^{-1} \frac{P_{beam}}{\text{MW}} D_y \frac{\mu\text{m}}{\sigma_z}$$

Higher luminosity thus requires a higher vertical disruption parameter, a shorter bunch or more beam power. Since TESLA has the longest bunch it also has the highest disruption parm For this reason, TESLA has the highest disruption parameter, followed by NLC and CLIC.

3 SIMULATION PROCEDURE

During the transport from the damping ring to the IP the emittances of the beam are increasing due to imperfections of the beamlines. One attempts to minimise this growth by the use of different emittance preservation methods, e.g. beam-based alignment of the magnets in the main linac. Since a residual growth will remain, all projects specify an emittance growth budget, see table 2. In the following it should be investigated, if, in spite of the bananan effect, the emittance budgets are consistent with the specified luminosities, which are simulated without taking the correlations in the beams into account. Therefore one needs to generate this emittance growth in the simulation of the beam transport from the damping ring to the IP.

The different correction procedures have not been specified in detail for all the different subsystems, which transport the beams; most effort has been spent on the main

linacs. For the simulations therefore the following simplification is made. No emittance growth due to imperfections is assumed before or after the main linac. In the linac an emittance growth is produced that is equivalent to the full budget. As soon as more detailed correction procedures become available for the other sub-systems, further studies will needed to include their effect.

Different computer codes can be used to simulate the beam-based alignment of the main linac [3, 4, 5]. However, the different projects use different beam based alignment techniques and different tracking codes. The comparison of these codes is progressing but not yet completely satisfying. Therefore a simplification is made in the simulation of the main linac alignment. Artificial initial misalignments of the accelerating structures and beam-position monitors (BPMs) have been chosen by each project such that after the use of a simple one-to-one correction the remaining emittance growth corresponds to the emittance budget, see table 1. Consequently, most of these misalignments are much smaller than what could be tolerated if a full-fledged beam-based alignment procedure were used. The relative size of the errors was however carefully chosen in the simplified model to reflect the relative contributions to the emittance growth which can be expected from the realistic errors and full beam-based alignment. In the horizontal plane the emittance growth is not simulated but the value foreseen at the IP is used at the entrance of the main linac and no further imperfections are assumed. This is motivated by the fact that the static horizontal emittance growth in the linac should be of the same order as the vertical but the budget is much larger. In addition deviations of the horizontal emittance from the nominal one require adjustment of the horizontal beta-functions to keep σ_x and consequently the beamstrahlung constant.

The beam delivery system (BDS) which transports the beam from the linac to the IP is assumed to contain no imperfections, consequently no correction method needs to be applied. However, the mean angle and position of the beams coming in from the linac is corrected to zero, before entering the BDS.

In the above fashion, 200 different machines are simulated with PLACET [5] using different random number generator seeds for the initial misalignments in each main linac. The collisions of the result 100 pairs of bunches are simulated with GUINEA-PIG [6] to determine the luminosity. Each collision is optimised in several steps to obtain maximum luminosity. First, the mean angle and position of each bunch is corrected to zero. In the second step, the relative offset of the two bunches is varied to maximise luminosity. Finally a vertical crossing angle is introduced between the two beams. This is effectively the same as introducing a linear correlation between the longitudinal and transverse position z and y in both beams. All these manipulations are performed by simply modifying the particle position and angles directly at the IP. No attempt is made to actually construct the tuning knobs which can modify the angle and the offset without introducing other effects.

Table 2: The emittances used (initial and final in the vertical plane) and the misalignments used to mimic the static errors of the machines. After application of the errors only a one-to-one correction was performed. If more sophisticated beam-based alignment schemes were used, much larger errors would be permitted.

	unit	TESLA	NLC	CLIC
ϵ_x	$[\mu\text{m}]$	10	3.6	2
$\epsilon_{y,i}/\epsilon_{y,f}$	$[\text{nm}]$	20/30	20/40	5/10
σ_{BPM}	$[\mu\text{m}]$	25	4.0	0.72
σ_{cav}	$[\mu\text{m}]$	500	10.0	8.0
σ'_{cav}	$[\mu\text{radian}]$	300	80	8.0

It is beyond the scope of this paper to design the appropriate systems for the different proposals. However, the offset correction can be easily achieved by corrector dipoles in the final doublets which would have deflection angles of only a few nanoradians. The crossing angle can easily be introduced by vertically deflecting crab crossing cavities, but a less local correction using dipoles before the final doublet should also be possible.

4 STATIC LUMINOSITY

Here, completely static machines are considered; the main focus is on TESLA since it has the highest disruption parameter. In reference [1], it was suggested that at least some of the luminosity lost due to the banana effect could be recovered by optimising the collision parameters, especially the relative offsets between the two beams and their crossing angle. More details and results can be found in [7].

4.1 Achieved Luminosities

In table 3 the target luminosities \mathcal{L}_0 as well as the ones achieved are shown for all designs. In the case of NLC and CLIC the luminosities \mathcal{L}_1 obtained after correction of bunch offsets and angles are not far from the target; optimisation of the offset results in a moderate increase in luminosity to \mathcal{L}_{off} . A smaller improvement to \mathcal{L}_{ang} is gained from the additional optimisation of the angle. The total improvement is about 20%. In the case of TESLA the optimisation of the offset yields a gain close to that obtained in the normal conducting machines. The angle optimisation however is very effective. The total gain of the optimisation is about 50%. In all cases, iterating the optimisation, starting from the optimum of the first one, does not significantly improve the results.

In all cases, the maximum luminosities achieved are close to the target values, in NLC and CLIC they are somewhat higher, in TESLA it is slightly lower. However, one should note that in TESLA the target luminosity was determined taking advantage of the improvement that can be obtained from a waist shift. The vertical focusing point of each beam lies not at the IP but $250 \mu\text{m}$ before it; this results in an increase of the luminosity from

	unit	TESLA	NLC	CLIC
\mathcal{L}_0	$[10^{34}\text{m}^{-2}\text{s}^{-1}]$	3.4	2.1	2.3
\mathcal{L}_1	$[10^{34}\text{m}^{-2}\text{s}^{-1}]$	2.2	1.8	2.2
\mathcal{L}_{off}	$[10^{34}\text{m}^{-2}\text{s}^{-1}]$	2.5	2.1	2.5
\mathcal{L}_{ang}	$[10^{34}\text{m}^{-2}\text{s}^{-1}]$	3.3	2.2	2.6

Table 3: Luminosities found for all machines. The target luminosities \mathcal{L}_0 quoted differ from the values quoted in [2] because there an additional luminosity reduction due to the tuning of the BDS is taken into account. This effect is neglected here.

$3.0 \times 10^{34} \text{ cm}^{-2}\text{s}^{-1}$ to about $3.4 \times 10^{34} \text{ cm}^{-2}\text{s}^{-1}$.

4.2 Luminosity Improvement by a Waist Shift

In reference [8] it was found that introducing a waist shift significantly increased the luminosity. The vertical focal point of each of the two beams is slightly upstream of the IP. The strong beam-beam interaction focuses the beams during the collision thus preventing the increase of the vertical beam size which would occur after the focal point if no forces were present.

To understand the influence of the banana effect on this, also the waist position of each beam was optimised. The improvement that was found is however very small. The mean improvement in the above cases is about 2%, in the best case it is 10%. Further study should establish whether the small improvement is due to the modification of the beam-beam interaction or due to the optimisation algorithm used, which optimised on parameter after the other not all simultaneously.

4.3 Luminosity as a Function of the Emittance Growth

For TESLA, the luminosity is shown as a function of the emittance growth in Fig. 1. It can be seen that even for very small emittance growth the luminosity can drop rapidly if only the beam positions and angles are zeroed. Offset and crossing angle between the two beams can be optimised to maximise the luminosity. The resulting luminosity is very close to the one expected from the simple scaling $\mathcal{L} \propto \sigma_y^{-1} \propto \epsilon_y^{-\frac{1}{2}}$.

One can conclude that for all machines the emittance budget foreseen seems appropriate, at least for static effects.

5 DYNAMIC SIMULATIONS

Dynamic banana effects are of special concern since they may be too fast to allow the above described luminosity optimisation. One of the main source of dynamic imperfection of the colliders is ground motion, which will be investigated in the following. Also some results for quadrupole jitter will be mentioned. Similar simulations of the effects of ground motion have been performed by A. Seryi et al.;

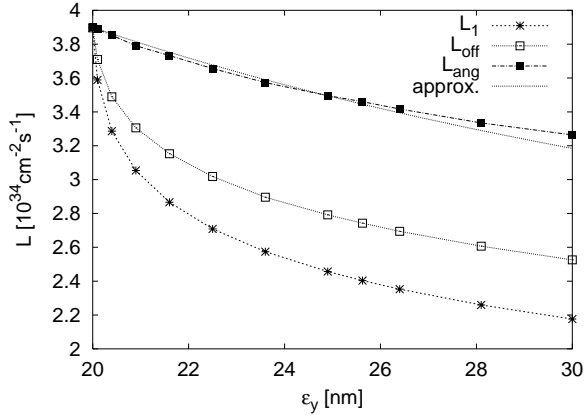


Figure 1: The luminosity as a function of the emittance at the end of the linac in the case of TESLA. For \mathcal{L}_1 the mean angle and position are zeroed in each beam, for \mathcal{L}_{off} the offset between the two beams was optimised to yield maximum luminosity. Finally, for \mathcal{L}_{ang} also the crossing angle was optimised. For comparison, the expected luminosity using the simple scaling $\mathcal{L} \propto \epsilon_y^{-\frac{1}{2}}$ is also shown.

they and more detailed results of the present paper will be published soon in a common report [9].

5.1 Ground Motion

The ground motion is simulated using a model developed by A. Seryi [10]; it takes into account the correlation in space and time. Three different sites are investigated, a very quiet one (measured in the LEP tunnel at CERN), a slightly more noisy one (measured in the SLAC tunnel) and a noisy one (measured in the HERA tunnel). For consistency with [2] they are named A, B and C, respectively.

5.2 Simulation Procedure

The simulation of the dynamic effects is based on the same corrected machines used above. First, full correction and optimisation of the beam collision parameters is performed neglecting all dynamic effects. In the simulation the ground motion moves the girders which support the beamline elements. The girders are assumed to be completely rigid in the following. Their lengths in the main linac are taken from data made available for the ILC-TRC [2]. In the beam delivery system each element is assumed to be on a separate girder. In some cases it was necessary to join a number of elements from the MAD decks because they represent a single real element, e.g. a combination of a half quadrupole a beam-position monitor and another half quadrupole is quite common. The ends of the girders are moved by the ground motion which in turn move the elements. In order to model the slow trajectory feedbacks in an approximate fashion it is assumed that the position y_i of each element is corrected from one pulse to the next by $\Delta y_1 = -g \times y_i$, where g is assumed to be representative of the gain of the slow feedbacks. All machines are left

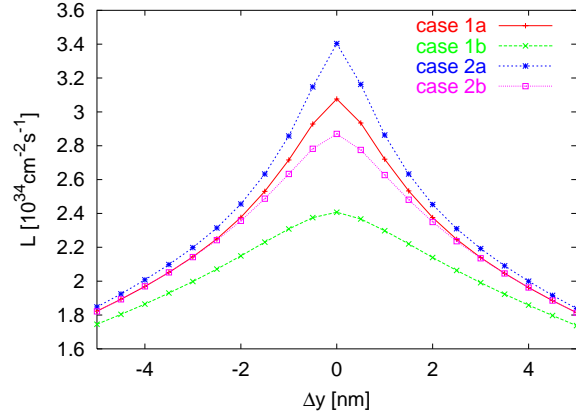


Figure 2: The luminosity as a function of the offset for different cases, see text.

running for 500 pulses to achieve convergence of the slow feedbacks before the fast feedback is switched on.

At least in the normal conducting machines the final quadrupoles will be stabilised; a number of investigation of possible approaches is ongoing [11, 12]. Most of the motion close to the IP may be due to technical noise sources, e.g. the detector itself. The reduction of the quadrupole motion is system as well as site dependent. A concise estimate of the movements needs detailed technical investigations and can not be attempted in this paper. Here, a simplified approach is chosen; the quadrupoles are perfectly stabilised. This is optimistic but a great effort is expected to be put into the stabilisation of the final quadrupoles, so that one can expect excellent performance of these systems, in spite of the fact that they will be in a difficult environment close to the detector—or even inside.

5.3 Beam-Beam Simulation Effects

Especially with high disruption, the sensitivity of the luminosity to dynamic effects depends on the initial value achieved. This is illustrated by the following calculation. For TESLA 25 machines are simulated using the full misalignments from table 2 (case 1) and half of these misalignments (case 2). For each of these cases the luminosity is maximised by optimising the offset (case 1a, case 2a) and by optimising the offset and angle of the beams (case 1b, case 2b). Figure 2 shows the luminosity loss for each of these cases as a function of the deviation Δy of the beam-beam offset from the optimum one. For $\Delta y = 0$ the absolute luminosities are quite different. For larger $|\Delta y|$ the difference in luminosities are reduced. The improvement obtained by the optimisation is lost. For the same relative luminosity loss, the offset tolerance is tighter in the better optimised case than in the less optimised one. The degree of luminosity optimisation can critically affect the sensitivity to offsets.

In the case of TESLA the target luminosity was not fully achieved using the full emittance growth budget. To obtain the relevant sensitivity to the dynamic offsets it seems

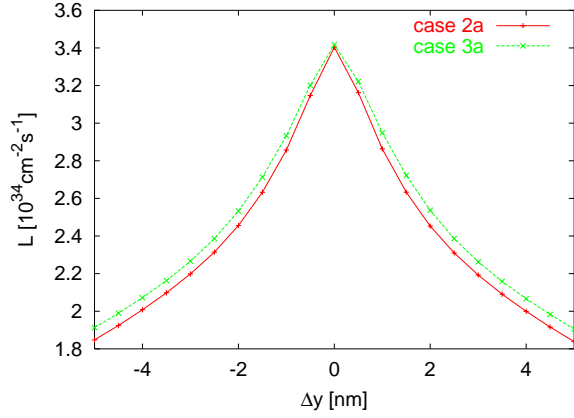


Figure 3: The luminosity as a function of the offset. In the second case more slices and macro particles were used in the beam-beam simulation and larger misalignments were applied in the main linac.

therefore necessary to scale the misalignments of the static machines such that the full luminosity is actually achieved. As a cross check that this is a reasonable approach, the following simulation is performed. First, the misalignments are scaled down to 50% and the beam-beam interaction is simulated using 24 timesteps and 24000 macro particles. This yields the target luminosity. Second, 85% of the misalignments are applied and the beam-beam simulation is performed using 72 timesteps and 72000 particles. This also yields the target luminosity. The luminosity as a function of the difference of the beam-beam offset to the optimum value is shown in Fig. 3. The dependence on the offset is very similar in both cases. In the following simulations, 24 timesteps and 24000 particles are used to speed them up. Better resolution will become necessary as the simulations become more detailed.

5.4 IP-Feedback Layout

Different fast interaction-point feedbacks are considered. The angle feedback uses some BPMs which are located $(n * 180 + 90)^\circ$ from the interaction point to determine the angle of the incoming beam at collision. The position feedback uses one or more BPMs after the collision to determine the beam offsets. If the beams collide even with a small offset at the interaction point, each of them is strongly kicked by the oncoming beam. For an offset of a 1 nm the typical deflection angle is $\mathcal{O}(10 \mu\text{rad})$ which leads to an easily measurable offset at the BPMs. These feedbacks can either act from pulse to pulse and in TESLA even within a pulse from bunch to bunch. Also in the normal conducting machines, a correction of the beam-beam offset within a pulse may be feasible, but is technically challenging since the duration of each pulse is only of the order of 100–300 ns. The feedback latency, caused by the time of flight between IP and BPM and correction kicker and IP as well as the response time of the electronics, is thus not negligible.

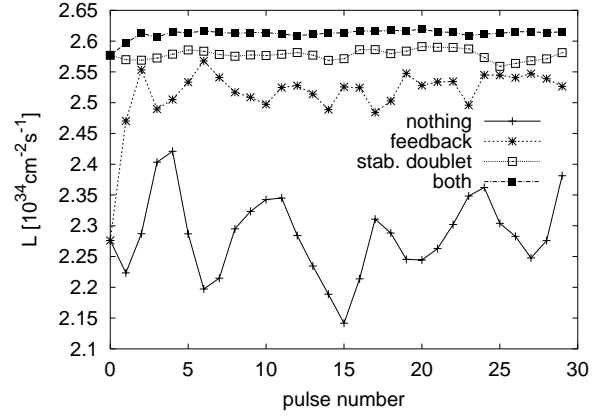


Figure 4: The luminosity as a function of the pulse number in the case of CLIC. The intermediate ground motion model B is used.

In the case of TESLA one can even hope to not only be able to correct but to rather optimise the collision offset and the beam angles within a pulse, by maximising the signal of a fast luminosity monitor. Such a fast monitor could be a pair monitor [13], which takes advantage of a background signal. While the signal of this monitor is not strictly proportional to the luminosity, its maximisation yields maximum luminosity. The hardware layout and the precision of this monitor and the exact algorithm of this challenging optimisation need to be studied.

5.5 Inter-Pulse Feedback Simulations

As described above, in the simulation of the inter-pulse feedback the beamline is first left running for 500 pulses with the slow feedbacks only. Then the fast interaction point feedback is switched on. When it has converged the following 20 pulses are averaged to determine the luminosity. All results are averaged over 25 different machines, each machine has a different seed for the random number generator used in the simulation of the ground motion.

Figure 4 shows the luminosity in CLIC as a function of the pulse number for ground motion model B. Without the IP feedback the luminosity remains about constant. Perfect stabilisation of the final doublets leads to significantly higher luminosity; as expected almost all the luminosity loss is due to the motion of these magnets. If the quadrupoles are not stabilised but the IP feedback is switched on, the luminosity also increases significantly. It does not quite reach the level obtained with the quadrupole stabilisation but comes close. The combination of stabilisation and IP feedback finally yields the best results.

The luminosity losses for the different types of ground motion are shown in table 4 for CLIC and NLC. Even in the very noisy site corresponding to model C a significant fraction of the luminosity remains. But the RMS fluctuation of the luminosity from pulse to pulse is quite large. In order to be able to measure the luminosity with a reasonable resolution of a percent requires some hundred pulses. In

Table 4: The relative luminosity loss Δ due to ground motion in percent for NLC and CLIC using a pulse-to-pulse feedback. The RMS luminosity variation σ of consecutive pulses is also given in percent. Values are either with no stabilisation (no stab.) or with stabilisation (stab.) of the final doublet. Slow feedbacks were running with a gain $g = 0.04$ all the time. These numbers were calculated to cross check results obtained by A. Seryi [9]. While the simulations are somewhat different, the agreement of the results is reasonable but not perfect.

Model	NLC				CLIC			
	no. stab.		stab.		no. stab.		stab.	
	Δ	σ	Δ	σ	Δ	σ	Δ	σ
A	0.1	0.1	0.1	0.1	0.1	0.1	0.1	0.1
B	4.3	4.4	0.5	0.7	3.8	4.3	0.3	0.4
C	42	32	23	17	69	80	40	22

Table 5: The relative luminosity loss in NLC and CLIC if an intra-pulse position feedback is used. The time needed by the feedback to converge is neglected. Different gains g for the slow feedbacks are assumed.

model	NLC		CLIC	
	$g = 0.01$	$g = 0.04$	$g = 0.01$	$g = 0.04$
A	0.1	0.1	0.1	0.1
B	0.1	0.1	0.3	0.15
C	6.7	6.6	30	28

the case of the more quiet models A and B, the fluctuations are much smaller and the number of pulses over which one needs to integrate is likely dominated by the resolution of the luminosity monitor.

5.6 Intra-Pulse Feedback

For the simulations of the intra-pulse feedback, as in the calculations before, the machine is left running for 500 pulses with the slow feedbacks only. Then the intra-pulse feedback is switched on. The luminosity quoted is the one found for the steady state after the feedback has converged. In the case of the normal conducting machines the latency time of the offset and angle feedback is not negligible compared to the length of the pulse. Already the intra-pulse angle feedback may be too difficult to be realised. A luminosity based optimisation of the collision within a pulse seems excluded. Table 5 shows the relative luminosity loss for the three different ground motion models. It is assumed that only the offset is corrected by the interaction point feedback, while the angle is corrected with the slower feedbacks. As can be seen, the gain used for the slow feedbacks is not important. The luminosity loss is noticeable only in the presence of strong ground motion. If one could apply full optimisation within the pulse (which one cannot) the luminosity loss would, for ground motion model C, be reduced to 4.4% for NLC and 22% for CLIC; not a large gain.

In the case of TESLA the long pulse duration may allow one to perform the full luminosity optimisation within the

Table 6: Percentage of luminosity lost in TESLA in the presence of ground motion according to model C, using an intra-pulse feedback. The effect of a BPM based correction of the beam-beam offset as well as of the offset and angle is shown first. Also the results obtained with a luminosity monitor based optimisation of offset as well as offset and angle is given. In the case of full optimisation, the slow feedbacks have a significant impact on the luminosity loss.

correction applied	slow feedback gain			
	0.01	0.02	0.04	0.1
No feedb.	73	71	67	56
offset correction	36	33	29	26
+angle correction.	22	19	16	15
offset optimisation	15.1	11.7	9.3	7.8
+angle optimisation	10.4	7.3	5.7	4.6

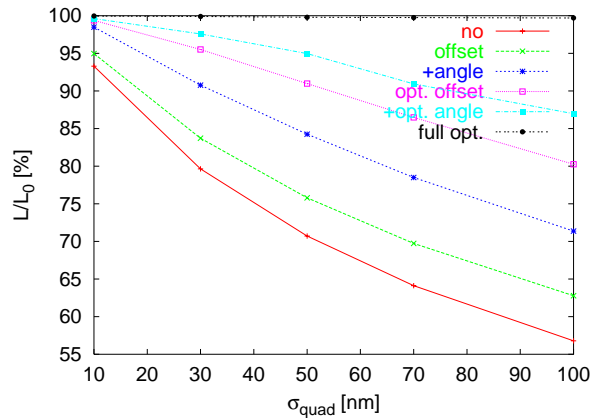


Figure 5: The luminosity loss as a function of the main linac RMS quadrupole jitter in TESLA.

pulse. A detailed study of such a feedback remains to be done. The relative luminosity achievable using the intra-pulse feedbacks and optimisation is given in table 6. As can be seen, already the offset minimisation leads to a significant improvement of the luminosity. A smaller but still noticeable gain is obtained by the angle feedback. Use of the luminosity monitor for optimisation gives further improvements. In these cases the effect of the slow feedbacks is very visible. Their gain is more important in TESLA than in the normal conducting designs, mainly because the time between pulses is longer. Consequently the magnets, especially the ones other than the final doublet, move more between pulses.

While in the normal conducting designs an intra-pulse luminosity monitor would result in a small benefit, the obtained gain can be significant in TESLA making such a device very desirable.

5.7 Jitter Effects in the TESLA Linac

Another potential source of beam jitter is transverse jitter of the main linac quadrupoles. To estimate the impact on the luminosity in TESLA, the following simulation

was performed. In each of the corrected machines used for the ground motion simulations, the linac quadrupoles were randomly misaligned while the beam delivery system was assumed to remain perfect. It was assumed that the quadrupoles only move from one pulse to the next but not during a pulse. While this is not strictly true it should be a good approximation; a motion within the pulse which is slow compared to the bunch frequency can be cured within a train. Different intra-train feedback configurations were considered. A quadrupole jitter of 100 nm leads to an emittance growth in the linac of the order of 1% and lets the beam trajectory jitter by about $1\sigma_y$.

Figure 5 shows the luminosity as a function of the quadrupole jitter. In case no correction is performed more than 40% of the luminosity are lost for a jitter of 100 nm. A small improvement is obtained if the beam offset at the IP is corrected using the BPMs. But even an additional BPM based angle correction leaves a loss of 30%. If in addition an optimisation of the offset or angle and offset at the IP is performed further improvement can be obtained but a loss of 13% remains, which is larger than what one expects from the emittance growth in the main linac. This indicates an additional emittance growth in the BDS due to the trajectory oscillation. As expected, the use of an additional intra-pulse feedback before the BDS which steers the beam to its original trajectory can reduce the luminosity loss to about 0.5%.

6 CONCLUSION

One can conclude that, in spite of the strong beam-beam effects, one should be able to achieve the target luminosities in all linear colliders discussed by respecting the foreseen emittance budgets. This requires full maximisation of the luminosity by optimising the collision offset and angle. However, the impact of dynamic effects on the optimisation procedure remains to be investigated.

Using pulse-to-pulse feedback, the normal conducting machines have little luminosity loss if the ground motion is equivalent to model A or B—and if the final doublet quadrupoles are stabilised in the latter case. Strong ground motion (model C) leads to significant luminosity loss. An intra-train feedback may recover a good part of this in the NLC and a significant fraction in CLIC but is technically very challenging.

In the case of TESLA intra-pulse feedback can certainly be used. In case of severe ground motion (model C) the luminosity loss can however still be large. A fast pulse-to-pulse orbit feedback can significantly reduce this loss. Also a fast intra-pulse luminosity optimisation is very desirable since it gives a significant further improvement. Such an optimisation seems however very challenging.

Stabilisation of magnets other than the final doublets may improve the situation in all machines.

Quadrupole jitter leads to small emittance growth but significant motion of the beam trajectory in the main linac of TESLA. While here the intra-pulse IP feedback also im-

proves the performance, a residual luminosity loss remains even after luminosity optimisation. It can be almost completely cured by the use of an intra-pulse trajectory feedback before the beam delivery system.

In all cases a more detailed study of the feedbacks seems necessary, especially to better understand the interplay of different feedback systems. Further study is required to establish that the effect of static imperfections can be tuned out in a dynamically moving machine.

7 ACKNOWLEDGMENT

The author wants to thank A. Seryi for useful discussions and for helping to make the ground motion models available in PLACET. P. Tenenbaum, N. Walker and M. Woodley helped by answering many detailed questions concerning the NLC and TESLA lattices.

8 REFERENCES

- [1] R. Brinkmann, O. Napoly and D. Schulte. "Beam-Beam Instability Driven by Wakefields." CLIC-Note 505 (2001).
- [2] The International Linear Collider Technical Review Committee is headed by G. Loew. The review should be published early 2003.
- [3] R. Assmann, et al. The Computer Program LIAR for the Simulation and Modeling of High Performance Linacs.
- [4] MERLIN was written by N. Walker, see <http://www.desy.de/merlin>.
- [5] E. D'Amico, G. Guignard, N. Leros, D. Schulte. "Simulation Package based on PLACET." 2001 Particle Accelerator Conference (PAC'2001), Chicago, Illinois, USA, June 18-22, 2001 and CERN/PS 2001-028 (AE).
- [6] D. Schulte. "Beam-Beam Simulations with Guinea-Pig." ICAP98, Monterey, CA., USA, September 1998 and CERN/PS 99-014 (LP).
- [7] D. Schulte. "Luminosity in Future Linear Colliders in the Presence of Static Wakefield Effects in the Main Linac". To be published as CLIC-Note 544 (2002).
- [8] D. Schulte. "Study of Electromagnetic and Hadronic Background in the Interaction Region of the TESLA Collider." PhD. thesis. TESLA 97-08 (1996).
- [9] D. Schulte, A. Seryi et al. To be published.
- [10] A. Seryi. PAC 2001, Chicago, Illinois, USA.
- [11] R. Assmann, W. Coosemans, G. Guignard, N. Leros, S. Redaelli, W. Schnell, D. Schulte, I. Wilson, F. Zimmermann. Status of the CLIC Study on Magnet Stabilization and Time-Dependent Luminosity CERN/SL 2002-046 (AP).
- [12] J. Frisch. These proceedings.
- [13] O. Napoly and D. Schulte, "Luminosity Monitor Options For Tesla," CERN-OPEN-2000-135 *Contributed to 19th International Linear Accelerator Conference (Linac 98), Chicago, Illinois, 23-28 Aug 1998.*